



GPR109a agonists. Part 1: 5-Alkyl and 5-aryl-pyrazole–tetrazoles as agonists of the human orphan G-protein coupled receptor GPR109a

Jason E. Imbriglio^{a,*}, Sookhee Chang^a, Rui Liang^a, Subharekha Raghavan^a, Darby Schmidt^a, Abby Smenton^a, Scott Tria^a, Thomas O. Schrader^c, Jae-Kyu Jung^c, Craig Esser^a, Andrew K. P. Taggart^b, Kang Cheng^b, Ester Carballo-Jane^b, M. Gerard Waters^b, James R. Tata^a, Steven L. Colletti^a

^a Department of Medicinal Chemistry, Merck Research Laboratories, Merck & Co., Inc., PO Box 2000, Rahway, NJ, 07065-0900, United States

^b Department of Cardiovascular Diseases, Merck Research Laboratories, Merck & Co., Inc., PO Box 2000, Rahway, NJ, 07065-0900, United States

^c Department of Medicinal Chemistry, Arena Pharmaceuticals, 6166 Nancy Ridge Drive, San Diego, CA 92121, United States

ARTICLE INFO

Article history:

Received 24 February 2009

Revised 4 March 2009

Accepted 4 March 2009

Available online 9 March 2009

Keywords:

Niacin

GPR109a

Atherosclerosis

ABSTRACT

5-Alkyl and aryl-pyrazole–tetrazoles have been identified as a new class of selective, small-molecule, agonists of the human G-protein-coupled receptor GPR109a, a high affinity receptor for the HDL-raising drug nicotinic acid.

© 2009 Elsevier Ltd. All rights reserved.

Nicotinic acid (niacin) **1** has been a leading treatment for dyslipidaemia and for the prevention of atherosclerosis for over 40 years.¹ Long term clinical studies have revealed niacin's ability to reduce mortality from coronary heart disease.² In spite of niacin's clinical significance, patients treated with niacin show low compliance of use due to an intense flushing side effect.^{3,4} A number of drug discovery programs have focused on the development of a 'flush-free' niacin-like therapy. Despite considerable effort in the field, the absence of a niacin-related target and/or mechanism of action have limited such investigations.

Recently, a G-protein-coupled receptor, GPR109a, was identified as a molecular target for niacin.⁵ Mechanistic studies have suggested that the benefits of niacin therapy may result from the activation of GPR109a located on adipocytes.⁶ Recent experiments have shown that niacin activation of GPR109a results in a reduction of intracellular cAMP and it is believed that this reduction in cAMP levels effectively inhibits lipolysis by the negative modulation of hormone sensitive lipase (HSL). As a result, a concomitant decrease in plasma free fatty acid (pFFA) levels is observed and it is thought that this reduction in pFFA is crucial to the lipid modulation and resulting therapeutic value of niacin.⁷

In control experiments, GPR109a knockout mice, when treated with niacin therapy, failed to show the characteristic reduction in

plasma FFA that is observed in wild type mice. Furthermore, these mice also failed to show a niacin-induced cutaneous flush. As a result, it has been suggested that the niacin-associated flush and anti-lipolytic effects are both mediated through GPR109a.^{5a}

In light of these recent findings, we initiated a drug discovery program focused on the identification of a 'flush-free' agonist of the niacin receptor. Our lead identification effort identified pyrazole–tetrazole **2** as a promising candidate.^{8–10} While pyrazole **2** displayed only modest in vitro affinity for GPR109a (Table 1), its in vivo pharmacology was intriguing (see Fig. 1).¹¹

In a mouse plasma free-fatty acid (pFFA) assay, mice treated with 10 mpk of pyrazole **2** showed a net reduction in plasma free fatty acid levels comparable to that observed upon treatment with 100 mpk of niacin. Furthermore, in a mouse vasodilation-assay (mVD), mice treated with 30 mpk of **2** failed to show any signs of the characteristic cutaneous flushing response observed with niacin treatment. This putative decoupling of the free fatty acid and cutaneous flushing effect characteristic of niacin treatment captivated our attention. As a result, pyrazole **2** became the focal point of our medicinal chemistry effort.

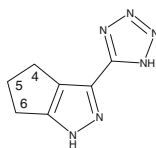
The initial goal of the program focused on improving the in vitro profile of pyrazole **2**. With this goal in mind, we proceeded to explore the SAR around the framework of pyrazole **2**. Early in our efforts, we discovered that both the pyrazole and tetrazole moieties were essential in retaining affinity for the receptor. In addition, it was discovered that substituents in either the C4 or C6 positions

* Corresponding author.

E-mail address: jason_imbriglio@merck.com (J.E. Imbriglio).

Table 1Agonism of GPR109a by C5-substituted pyrazole–tetrazoles^a

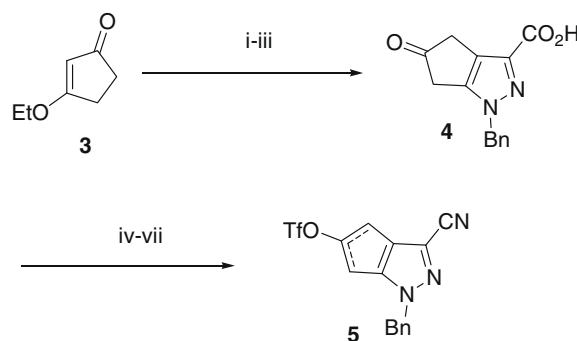
Compd	R ¹	R ²	IC ₅₀ ^b (μM)	
			mNBA	hNBA
1	—	—	0.14	0.14
2	H	Tetrazole	1.2	1.5
8a	Ethyl	Tetrazole	1.3	4.6
8b	<i>n</i> -Propyl	Tetrazole	0.26	0.69
8c	<i>n</i> -Butyl	Tetrazole	0.21	0.34
8d	<i>ent</i> - <i>n</i> -Butyl	Tetrazole	0.06	0.08
8e	<i>n</i> -Pentane	Tetrazole	3.6	4.8
8f	<i>n</i> -hexane	Tetrazole	0.8	0.87
8g	Cyclopropyl	Tetrazole	2.5	5.2
8h	Cyclopentyl	Tetrazole	9.0	2.5
9a	Ph	Tetrazole	0.31	0.43
9b	3-Me-Ph	Tetrazole	11.0	16
9c	2-Me-Ph	Tetrazole	4.2	7.7
9d	4-Cl-Ph	Tetrazole	4.0	5.0
9e	4-F-Ph	Tetrazole	1.7	2.7
9f	2,4-F-Ph	Tetrazole	1.6	2.4
9g	2,5-F-Ph	Tetrazole	0.85	0.76
9h	2-Cl-Ph	Tetrazole	3.1	1.9
9i	3,4-F-Ph	Tetrazole	0.52	0.61
9j	2,3-F-Ph	Tetrazole	0.09	0.14
9k	2-F-Ph	Tetrazole	0.34	0.41
9l	3-Cl-Ph	Tetrazole	0.14	0.29
9m	3-F-Ph	Tetrazole	0.08	0.14
9n	2,3,5-F-Ph	Tetrazole	0.07	0.08
9o	<i>ent</i> 2,3,5-F-Ph	Tetrazole	0.04	0.04
9p	3,5-F-Ph	Tetrazole	0.07	0.07

^a Values are an average of two or greater individual assays.^b [³H]-Nicotinic acid binding competition assay.**Figure 1.** Lead candidate pyrazole–tetrazole **2**.

of the saturated carbon backbone of **2** were poorly tolerated. In light of these observations, we focused our attention around the C5 position of the molecule.

In order to explore the C5 position of the molecule most judiciously, we utilized triflate **5** as a late stage synthetic intermediate that allowed for the installation of both alkyl and aryl substituents into the framework of the molecule. As outlined in Scheme 1, our synthesis toward compound **5** began with acylation of the commercially available cyclopentenone **3** followed by a condensation reaction with benzyl hydrazine to install the pyrazole. Hydrolysis of the enol-ether and *t*-butyl ester revealed ketone **4** which was further elaborated to the nitrile. Finally, the C5 ketone was converted to the desired enol-triflate intermediate **5**.

Enol-triflate **5** was converted to the desired C5-alkyl or C5-aryl substituted pyrazole **6** via Suzuki or Stille couplings with the appropriate boronic acid or organostannane. With the desired C5 substituent in place, the tetrazole functionality was furnished through a [3+2] cycloaddition with sodium azide to afford **7**. Finally, hydrogenation provided the saturated carbon backbone with

**Scheme 1.** Reaction conditions: (i) LDA, di-*t*-butyl oxalate; (ii) BnNHNH₂·HCl; (iii) TFA; (iv) NHS, EDC; (v) NH₄OH; (vi) cyanuric chloride; (vii) LDA, Comin's reagent.

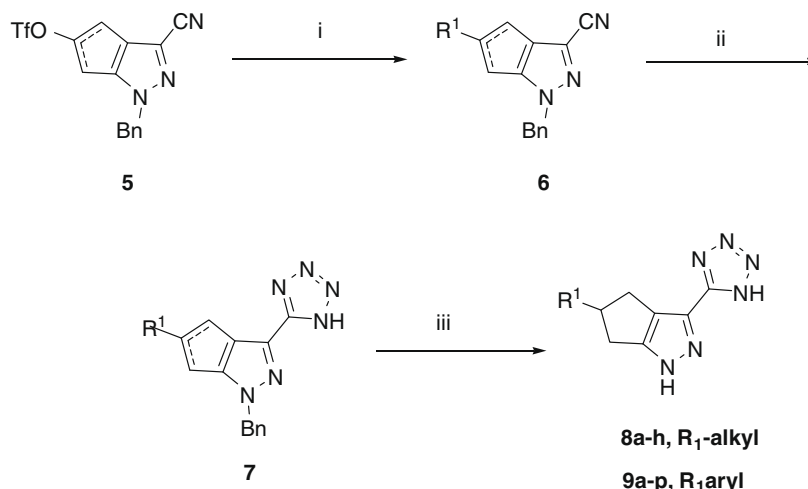
concomitant removal of the benzyl protecting group to afford the C5-pyrazole derivatives **8a–h** and **9a–p** (see Scheme 2).

As a means of identifying compounds suitable for in vivo analysis, we explored the in vitro activity of this class of pyrazole–tetrazoles. As illustrated in Table 1, the C5-alkyl-pyrazoles showed a markedly improved affinity for both the human (GPR109a) and murine (Puma-G) variants of the receptor. Ethyl derivative **8a** (1.3 μM and 4.6 μM) demonstrated nearly comparable in vitro affinity to pyrazole **2**, while propyl derivative **8b** (0.26 μM and 0.69 μM) provided a modest boost in potency with both the mouse and human receptors. Further extension of the carbon side-chain, as in *n*-butyl derivative **8c** (0.21 μM and 0.34 μM), showed an incremental boost in affinity as the racemate; however, a chiral resolution of **8c**, yielding the active stereoisomer **8d** (0.06 μM and 0.08 μM)¹² provided the most potent agonist within the C5-alkyl series. Additional elongation of the alkyl chain, as in pentane derivative **8e** (3.6 μM and 4.8 μM) and hexane derivative **8f** (0.8 μM and 0.87 μM) showed a precipitous drop in affinity, when compared to **8d**.

The saturated carbocyclic derivatives, pyrazoles **8g** (2.5 μM and 5.2 μM) and **8h** (9.0 μM and 2.5 μM), provided little improvement in potency when compared to the linear alkyl derivatives, whereas the C5-phenyl derivative **9a** (0.31 μM and 0.43 μM) showed promise as a scaffold for further structural modifications.

In this regard, a positional scan of a variety of functional groups on the phenyl ring system of **9a** exposed a tight binding pocket within this region of the molecule.¹³ It was discovered that phenyl rings bearing small alkyl groups or halogens were tolerated in this locale. As illustrated in Table 1, the methyl substituted ring systems **9b** (11 μM and 16 μM) and **9c** (4.2 μM and 7.7 μM) showed modest affinity for the receptor across both species, while halogen substitution about the phenyl ring showed improved in vitro potency. In particular, the placement of either a fluoro or chloro group in the 3-position of the phenyl ring as in **9l** (0.14 μM and 0.29 μM) and **9m** (0.08 μM and 0.14 μM) resulted in a significant improvement in potency. Whereas, substitution of a chloro group in either the 2 or 4-position as in **9h** (3.1 μM and 1.9 μM) and **9d** (4.0 μM and 5.0 μM) or a fluoro group as in **9k** (0.34 μM and 0.41 μM) and **9e** (1.7 μM and 2.7 μM) provided only a marginal improvement in potency. Amongst the disubstituted derivatives, the 3,5-fluoro derivative **9p** (0.7 μM and 0.7 μM) demonstrated improved affinity over the 2,4-difluoro derivative **9f** (1.6 μM and 2.4 μM), 2,5-derivative **9g** (0.85 μM and 0.76 μM) 3,4-derivative **9i** (0.52 μM and 0.61 μM) and 2,3-derivative **9j** (0.09 μM and 0.14 μM). Further fluoro substitution, as in enantiomer **9o** of the 2,3,5-trifluoro derivative **9n** proved to be the most potent compound in the C5-aryl-series.

In order to set the stage for in vivo analysis, mouse pharmacokinetics (mPK) of lead candidates were investigated (Table 2). In



Scheme 2. Reaction conditions: (i) $R^1B(OH)_2$, $Pd(PPh_3)_4$; (ii) NaN_3 , $ZnBr_2$; (iii) H_2 , $Pd-C$.

the alkyl series, *n*-propyl derivative **8b** showed a lower clearance (30 mL/kg/min), longer half life (2.9 h), and an improved bioavailability (51%), when compared with niacin. In contrast, compound **8d**, with better in vitro affinity than **8b**, demonstrated an inferior mPK profile when compared with **8b**.

Within the aryl series of molecules, the fluoro-derivative **9m** showed improved mPK with good bioavailability (57%), lower clearance (47 mL/kg/min) and a longer half-life (1.8 h) when compared with niacin. Similarly, the 2,3,5-trifluoro-derivative **9o** showed a longer half-life (2.4 h) and lower clearance (27 mL/kg/min) with a modest bioavailability (10%).

With a promising group of GPR109a agonists in hand, we were eager to investigate this new series of C5-substituted pyrazole-tetrazoles in an in vivo setting. In this effort, we chose to explore the pharmacology of **9o** in our mouse pFFA and mouse vasodilation assay. As illustrated in Figure 2, six male C57 B1/6 mice were each dosed at 10 mpk for 15 min with **9o** and compared to mice dosed 100 mpk with niacin for an effect on plasma free-fatty acids. In the case of compound **9o**, we observed a characteristic 24% reduction in plasma free fatty acid levels, while niacin, dosed at 100 mpk, showed a characteristic 58% reduction of plasma free fatty acids.

Having demonstrated the ability of agonist **9o** to effectively lower plasma free fatty acids in our mouse pharmacodynamics model, we proceeded to measure the cutaneous vasodilation effect of **9o** on male C57 B1/6 mice, as a surrogate for the flushing side effect experienced with niacin treatment. In this effort, compound **9o**, administered to 8 mice at 30 mpk for 15 min monitored with a laser doppler imager, showed no evidence of cutaneous flushing (Fig. 3).

While nicotinic acid (NA), administered in 10 mice at 30 mpk showed, on average, a characteristic 80% change in perfusion, typical of a flushing response in the mouse.¹⁴

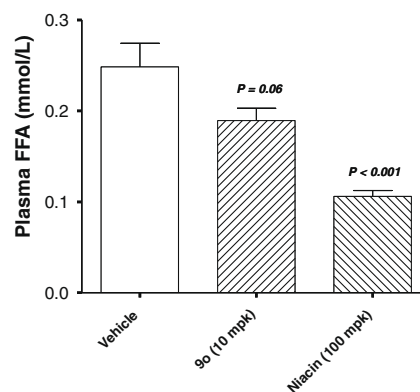


Figure 2. Mouse pFFA reduction studies.

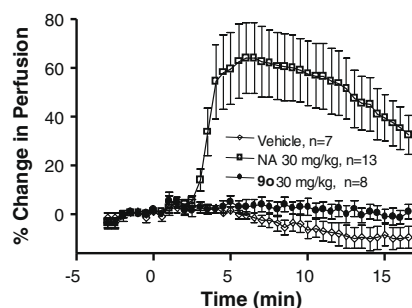


Figure 3. Mouse vasodilation studies.

Table 2
Mouse^a pharmacokinetics of pyrazole-tetrazoles

Compds	F ^b (%)	Cl _p (mL/kg/min)	Vdss (L/kg)	t _{1/2} ^c (h)
1	100	145	1.0	0.02
8b	51	30	1.55	2.9
8d	34	21	0.70	1.5
9m	57	47	1.79	1.8
9o	10	27	1.1	2.4

^a C57BL/6-mice.

^b Dose: 1 mg/kg iv; 2 mg/kg po.

^c t_{1/2} = plasma half-life (0–8 h).

In summary, we have identified a new class of C5-alkyl and aryl-pyrazole-tetrazoles that act as agonists of GPR109a. We proceeded to show that selected members of this family of compounds have improved mouse pharmacokinetic profiles when compared to niacin. Most notably, as part of an effort to identify and develop a flush-free niacin-like agonist of GPR109a, we have shown that agonist **9o** effectively reduces plasma free-fatty acids without eliciting a niacin-like flush in our mouse model. Current efforts are focused on further pre-clinical validation of the pyrazole-tetrazole series of GPR109a agonists.

Acknowledgment

The authors would like to thank Dr. Daniel Blom of Merck Research Labs for helpful discussions.

References and notes

- Carlson, L. A. *J. Int. Med.* **2005**, 258, 94–114.
- Tavintharan, S.; Kashyap, M. L. *Curr. Atheroscler. Rep.* **2001**, 3, 74.
- Knopp, R. H. *Am. J. Cardiol.* **2000**, 86, 51L–56L.
- For a discussion on the clinical use of the D₂ receptor antagonist laropripant as a means of suppressing the nicotinic acid-induced vasodilation in humans, refer to: Paolini, J. F.; Mitchel, Y. B.; Reyes, R.; Kher, U.; Lai, E.; Watson, D. J.; Norquist, J. M.; Meehan, A. G.; Bays, H. E.; Davidson, M.; Ballantyne, C. M. *Am. J. Cardiol.* **2008**, 101, 625.
- (a) Lorenzen, A.; Stannek, C.; Lang, H.; Andrianov, V.; Kalvinsh, I.; Schwabe, U. *Mol. Pharmacol.* **2001**, 59, 349; (b) Wise, A.; Foord, S. M.; Fraser, N. J.; Barnes, A. A.; Elshourbagy, N.; Eilert, M.; Ignar, D. M.; Murdock, P. R.; Steplewski, K.; Green, A.; Brown, A. J.; Dowell, S. J.; Szekeres, P. G.; Hassall, D. G.; Marshall, F. H.; Wilson, S.; Pike, N. B. *J. Biol. Chem.* **2003**, 278, 9869; (c) Soga, T.; Kamohara, M.; Takasaki, J. M.; Shun-Ichiro, S.; Tetsu, O.; Takahide, H.; Hideki, M. A.; Matsushime, H.; Furuichi, K. *Biochem. Biophys. Res. Commun.* **2003**, 303, 364.
- (a) Tunaru, S.; Kero, J.; Schaub, A.; Wufka, C.; Blaukat, A.; Pfeffer, K.; Offermanns, S. *Nat. Med.* **2003**, 9, 352–355; (b) Zhang, Y.; Schmidt, R. J.; Foxworthy, P.; Emkey, R.; Oler, J. K.; Large, T. H.; Wang, H.; Su, E. W.; Mosior, M. K.; Eacho, P. I.; Cao, G. *Biochem. Biophys. Res. Commun.* **2005**, 334, 729–732.
- Offermanns, S. *Trends Pharmacol. Sci.* **2006**, 27, 384.
- Identification of leads was based on the ability of compounds to decrease cAMP levels in forskolin-stimulated cells stably transfected with the niacin receptor (GPR109a).
- Van Herk, T.; Brussee, J.; van den Nieuwendijk, A. M. C. H.; van der Klein, P. A. M.; Ijzerman, A. P.; Stannek, C.; Burmeister, A.; Lorenzen, A. *J. Med. Chem.* **2003**, 46, 3945–3951.
- Semple, G.; Schrader, T.; Skinner, P. J.; Colletti, S. L.; Gharbaoui, T.; Imbriglio, J. E.; Jung, J. K.; Liang, R.; Raghavan, S.; Schmidt, D.; Tata, J. R. U.S. Patent, 2005.
- Semple, G.; Skinner, P. J.; Gharbaoui, T.; Shin, Y. J.; Jung, J. K.; Cherrier, M. C.; Webb, P. J.; Tamura, S. Y.; Boatman, P. D.; Sage, C. R.; Schrader, T. O.; Chen, R.; Colletti, S. L.; Tata, J. R.; Waters, G.; Cheng, K.; Taggart, A. K.; Cai, T. Q.; Jane, E. C.; Behan, D. P.; Connolly, D. T.; Richman, J. G. *J. Med. Chem.* **2008**, 51, 5105–5108.
- The enantiomer of 8 d showed only modest affinity for the receptor, 7 μ M (hNBA) and 5 μ M (mNBA) respectively, illustrating a clear stereochemical preference for groups substituted in this C5 position.
- A variety of functional groups including alkyl, naphthyl, trifluoromethoxy, trifluoromethyl, sulfonyl, and methoxy substituted ring systems were not tolerated in this region.
- Measured using a Periscan PIMII Laser Doppler Perfusion Imager system.